Asian Journal of Chemistry; Vol. 26, Supplementary Issue (2014), S299-S304

ASIAN JOURNAL OF CHEMISTRY

http://dx.doi.org/10.14233/ajchem.2014.19069

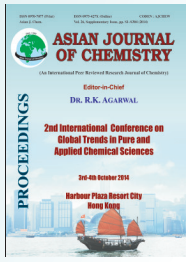

ab initio Density Functional Theory Calculations on Pyridoxine and Its Water Clusters

B. ATAK-BULBUL* and S. AKYUZ

Department of Physics, Istanbul Kultur University, Faculty of Science and Letters, Atakoy Campus, 34156 Istanbul, Turkey

*Corresponding author: Fax: +90 212 4658310; Tel: +90 212 4984176; E-mail: b.atak@iku.edu.tr

Published online: 24 December 2014; AJC-16494

The possible stable conformers of free pyridoxine molecule were searched by means of torsion potential energy surfaces scan studies through the dihedral angles, D1 (9H-8O-4C-3C), D2 (12H-10C-5C-6N), D3 (15O-14C-2C-1C) and D4 (O22-19H-3C-2C). The final geometrical parameters for the obtained stable conformers were determined by means of geometry optimization, carried out at DFT/B3LYP/6-311G++(d,p) theory level. Afterwards the possible pyridoxine-H_2O clusters were formed and their energetically preferred conformations were investigated using the same method and the same level of theory. The harmonic and anharmonic vibrational wavenumbers, IR and Raman intensities of the most stable monomer and water cluster were calculated. The assignment of the vibrational modes was performed based on the potential energy distribution of the vibrational modes, calculated by using GAR2PED program. Further, HOMO-LUMO energy gap was calculated.

Keywords: *ab initio* Calculations, Density functional theory, H_2O cluster, Pyridoxine, Vibrational spectra, Vitamin B_6.

INTRODUCTION

Vitamin B_6 plays a vital role in several enzymatic reactions. It acts as a coenzyme for numerous enzyme-catalyzed reactions such as transamination, α- and β-decarboxylations, β- and γ-eliminations, racemizations and aldol reactions[1]. Cinta *et al.*[2] investigated the pH dependence of the Raman and SERS spectra of pyridoxine hydrochloride and assigned the vibrational modes by the aid of *ab initio* (3-STO) and semi-empiric (PM3) calculations. Srivastava *et al.*[3] calculated the harmonic vibrational wavenumbers for the optimized geometry pyridoxine, using density functional theory method B3LYP/6-311++G** level of theory. But the geometry optimization was not performed by torsion potential energy surfaces scan studies through four the dihedral angles. It is well known that vibrational wavenumbers are strongly dependent on the conformational changes, for this reason, vibrational behavior of the lowest energy conformer of pyridoxine monomer was investigated. On the other hand up to our knowledge, no study has been reported on anharmonic wavenumbers or the H_2O clusters of pyridoxine. The aim of this study to give a complete description of the molecular geometry and molecular vibrations of pyridoxine in the framework of the density functional method both at harmonic and anharmonic levels and to investigate the hydrogen bonding interactions by modelling five different water complexes of the molecule. The experimental IR and Raman spectra of pyridoxine were also reported.

EXPERIMENTAL

The IR spectrum of the KBr disc of pyridoxine was recorded on a Bruker Tensor FT-IR spectrometer in the range 4000-400 cm^{-1} (0.5 cm^{-1} resolution). One hundred scans were accumulated. The FT-Raman spectra of pyridoxine was recorded on a BrukerMultiRam FT-Raman instrument using 1064 nm excitation from an Nd:YAG laser.

Computational part: The geometry optimizations and vibrational wavenumber (both harmonic and anharmonic) calculations of free pyridoxine molecule ($C_8H_{11}NO_3$) and five pyridoxine-H_2O complexes were carried out with the Gaussian 09 package[4]. Density functional theory method with Beckelyp functional[5] and 6-311++G(d,p) Pople *et al.*[6] basis set has been used. To reduce the big deviation between unscaled harmonic wave numbers and observed frequencies we were scaled all the wave numbers under 1800 cm^{-1} with the scale factor 0.98 and for over 1800 cm^{-1} the scale factor 0.955 for B3LYP/ 6-311++G(d,p) level of theory, respectively[7]. The potential energy distribution (PED) of the vibrational modes of the molecules was calculated with GAR2PED program[8]. The HOMO-LUMO energy gap was calculated using 6-311++G(d,p) basis set.

RESULTS AND DISCUSSION

The pyridoxine molecule consists of 23 atoms. The 63 normal modes of pyridoxine which span in the irreducible representation under C_1 point group have been established by the analysis of the experimental spectra.

Conformational analysis and H-bonding interactions: The molecular model of pyridoxine with the atom numbering scheme is given in Fig. 1. The scanned torsion angles (D1, D2, D3 and D4) are also shown in the Fig. 1. Stable low energy conformers of free pyridoxine molecule were obtained firstly by potential energy surface scan studies by iteratively varying D1 (9H-8O-4C-3C), D2 (12H-10C-5C-6N), D3 (15O-14C-2C-1C) and D4 (O22-19H-3C-2C) dihedral angles with step angle of 10°. The geometry optimization was then performed on the lowest energy conformer. The calculated geometrical parameters of the most stable conformer of pyridoxine are given in Table-1, in comparison with those of Srivastava *et al*[3]. As seen in Table-1, although our calculated values of bond lengths of the whole molecule and angles of the pyridine moiety are almost the same to those of Srivastava *et al.*[3], the dihedral angles are different, indicating that the conformations are not the same. In Table-1, the geometrical parameters different that those of Srivastava *et al*.[3] are given in bold.

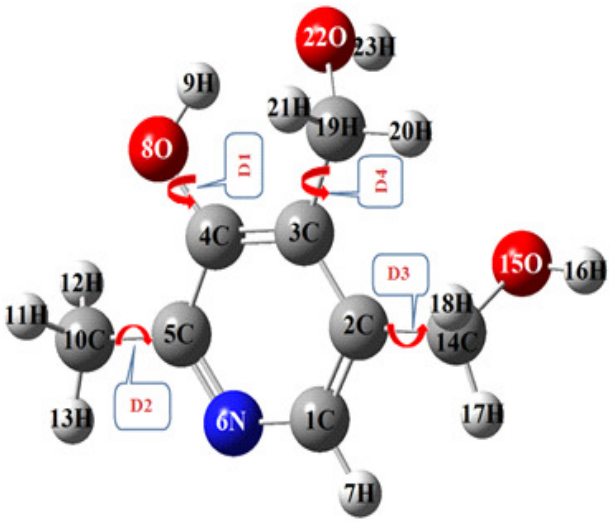

Fig. 1. Most stable geometry, atom numbering and searched dihedral angles of pyridoxine

TABLE-1
OPTIMIZED [DFT/6-311++G(d,p) LEVEL] BOND LENGTHS (R/Å), ANGLES(A/°) AND DIHEDRAL ANGLES (D/°) IN COMPARISON WITH THE RELATED DATA[3]

Bonding/structural parameters	This study	Ref. 3	Bonding angles	This study	Ref. 3	Bonding angles	This study	Ref. 3
R(1,2)	1.392	1.392	A(4,5,10)	120.331	120.197	**D(1,2,14,18)**	**-121.741**	**114.773**
R(1,6)	1.336	1.337	A(6,5,10)	118.635	118.625	**D(3,2,14,15)**	**-62.718**	**53.811**
R(1,7)	1.087	1.087	A(1,6,5)	118.961	118.874	**D(3,2,14,17)**	**176.657**	**172.213**
R(2,3)	1.405	1.407	**A(4,8,9)**	**108.429**	**111.072**	**D(3,2,14,18)**	**58.403**	**-64.280**
R(2,14)	1.506	1.511	**A(5,10,11)**	**111.121**	**109.258**	**D(2,3,4,5)**	**2.535**	**1.3291**
R(3,4)	1.399	1.399	A(5,10,12)	110.989	111.025	D(2,3,4,8)	-178.416	179.605
R(3,19)	1.512	1.514	A(5,10,13)	109.247	109.317	D(19,3,4,5)	-176.0280	176.251
R(4,5)	1.409	1.411	A(11,10,12)	106.550	106.519	D(19,3,4,8)	3.021	2.815
R(4,8)	1.363	1.362	A(11,10,13)	109.323	109.602	**D(2,3,19,20)**	**-111.003**	**14.824**
R(5,6)	1.333	1.332	**A(12,10,13)**	**109.563**	**108.439**	**D(2,3,19,21)**	**9.520**	**-105.414**
R(5,10)	1.503	1.593	**A(2,14,15)**	**109.065**	**111.323**	**D(2,3,19,22)**	**133.226**	**138.611**
R(8,9)	0.973	0.974	A(2,14,17)	108.888	109.972	**D(4,3,19,20)**	**67.477**	**-167.718**
R(10,11)	1.094	1.089	**A(2,14,18)**	**110.935**	**112.494**	**D(4,3,19,21)**	**-172.000**	**72.045**
R(10,12)	1.094	1.094	**A(15,14,17)**	**110.478**	**108.464**	**D(4,3,19,22)**	**-48.294**	**-43.931**
R(10,13)	1.089	1.089	A(15,14,18)	109.850	109.847	**D(3,4,5,6)**	**-1.572**	**-0.776**
R(14,15)	1.439	1.444	**A(17,14,18)**	**107.617**	**104.457**	D(3,4,5,10)	178.387	178.951
R(14,17)	1.095	1.094	A(14,15,16)	108.540	108.531	D(8,4,5,6)	179.334	-179.891
R(14,18)	1.098	1.089	**A(3,19,20)**	**110.043**	**111.802**	D(8,4,5,10)	-0.706	-0.163
R(15,16)	0.963	0.964	**A(3,19,21)**	**111.421**	**109.286**	D(3,4,8,9)	20.100	17.781
R(19,20)	1.094	1.092	**A(3,19,22)**	**112.130**	**113.013**	D(5,4,8,9)	-160.826	-163.126
R(19,21)	1.089	1.096	**A(20,19,21)**	**108.602**	**107.108**	**D(4,5,6,1)**	**-0.496**	**-0.286**
R(19,22)	1.444	1.436	A(20,19,22)	104.433	104.905	D(10,5,6,1)	179.544	179.982
R(22,23)	0.964	0.963	A(21,19,22)	109.935	110.517	D(4,5,10,11)	-60.598	-60.826
A(2,1,6)	124.152	124.196	A(19,22,23)	108.134	108.041	D(4,5,10,12)	57.779	178.501
A(2,1,7)	119.844	119.835	**D(6,1,2,3)**	**-0.539**	**-0.188**	D(4,5,10,13)	178.698	57.504
A(6,1,7)	116.003	115.971	D(6,1,2,14)	179.600	-179.285	D(6,5,10,11)	119.362	118.909
A(1,2,3)	117.811	117.836	D(7,1,2,3)	179.467	-179.986	D(6,5,10,12)	-122.261	-1.764
A(1,2,14)	119.606	119.647	**D(7,1,2,14)**	**-0.395**	**0.917**	D(6,5,10,13)	-1.342	-122.762
A(3,2,14)	122.583	122.510	**D(2,1,6,5)**	**1.579**	**0.781**	**D(2,14,15,16)**	**-176.507**	**-73.497**
A(2,3,4)	117.768	117.743	**D(7,1,6,5)**	**-178.423**	**-179.414**	**D(17,14,15,16)**	**-56.857**	**51.106**
A(2,3,19)	123.211	122.591	**D(1,2,3,4)**	**-1.517**	**-0.863**	**D(18,14,15,16)**	**61.715**	**167.259**
A(4,3,19)	119.004	119.620	D(1,2,3,19)	176.981	176.64	**D(3,19,22,23)**	**-69.108**	**-60.523**
A(3,4,5)	120.221	120.162	D(14,2,3,4)	178.340	178.206	**D(20,19,22,23)**	**171.768**	**177.431**
A(3,4,8)	122.237	122.566	**D(14,2,3,19)**	**-3.162**	**-4.291**	**D(21,19,22,23)**	**55.426**	**62.303**
A(5,4,8)	117.535	117.266	**D(1,2,14,15)**	**117.137**	**-127.136**	–	–	–
A(4,5,6)	121.033	121.177	**D(1,2,14,17)**	**-3.486**	**-8.734**	–	–	–

Solubility of a bioactive molecule is important. For this reason it is found to be interesting to study vibrational features of the water clusters of pyridoxine in comparison to its monomer form. All possible conformations of pyridoxine interacting with one water molecule and finely possible conformation of pyridoxine interacting five water molecules are determined. Fig. 2 demonstrates the geometries of the five stable pyridoxine-water clusters obtained using density functional theory method with B3LYP/6-311++G(d,p) basis set. The energies of the most stable monomer and energetically preferred H_2O-pyridoxine clusters are given in Table-2. As seen in Table-2, hydrogen bonding interactions with water molecules play an important role in stabilization of the molecule. Comparison of the geometric parameters of monomer form with those of water cluster of pyridoxine clearly shows the effects of inter molecular hydrogen bonding. The calculated hydrogen bonding distances are found to be 1.994-1.767 Å interval indicating the strong H-bonding interaction.

TABLE-2
CALCULATED ENERGIES OF PYRIDOXINE MONOMER AND PYRIDOXINE-H_2O CLUSTERS

Calculated energy (kcal/mol)	
Monomer	-371525.20
Cluster a	-419510.78
Cluster b	-419507.82
Cluster c	-419514.89
Cluster d	-419516.08
Cluster e	-563468.17

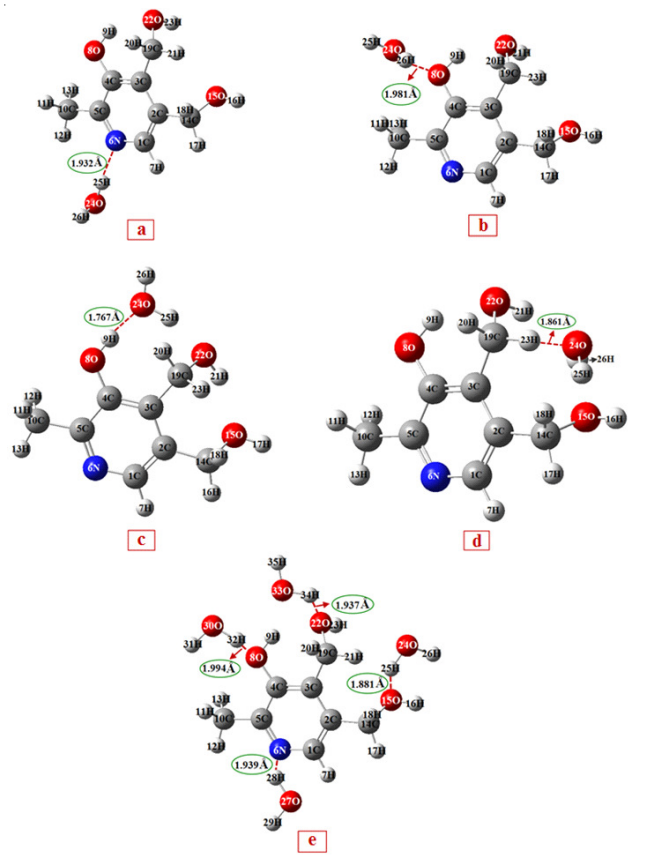

Fig. 2. Geometries of the five stable pyridoxine-water clusters obtained by of using density functional theory method with B3LYP/6-311++G(d,p) basis set and atomic numbering sheme

Vibrational analysis: The experimental FT-IR and Raman spectra of pyridoxine are given in Figs. 3 and 4, respectively. The calculated wavenumbers, the calculated Raman intensities and the potential energy distributions of the vibrational modes of pyridoxine are given in Table-3, in comparison with the experimental vibrational spectra of the investigated molecule. It is obviously seen that the anharmonic corrected wave numbers represent the whole experimental spectra very well. Pyridoxine-water cluster-a, represents hydrogen bonding interaction of pyridoxine through pyridine ring nitrogen (Fig. 2). Due to this interaction some ring modes of pyridine moiety altered. On the other hand pyridoxine-water cluster-e represents pyridoxine water solution well, in addition to some ring modes of pyridine moiety, CO stretching vibrations are altered. The altered wave numbers, due to hydrogen bonding interaction with water molecules are given in bold (Table-3).

HOMO-LUMO Analysis: HOMO and LUMO energies are very important parameters for quantum chemistry. The highest occupied molecular orbital (HOMO) energy characterizes the ability of electron giving, the lowest unoccupied molecular orbital (LUMO) energy characterizes the ability of electron accepting. In order to evaluate the energetic behaviour

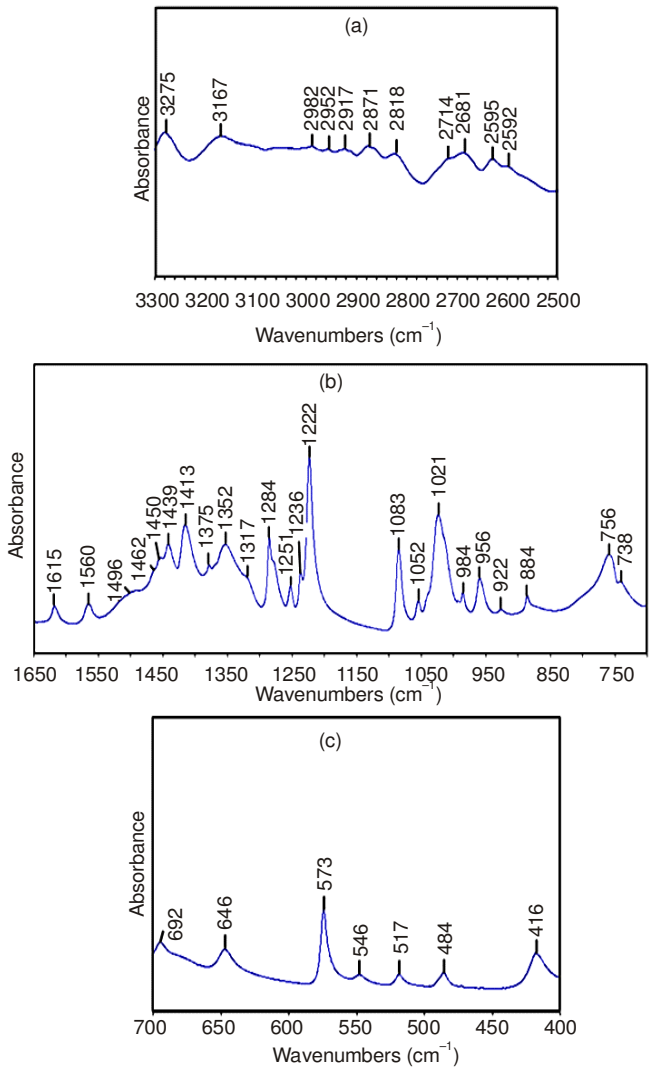

Fig. 3. Experimental FT-IR spectra of pyridoxine in the regions (a) 3300-2500 cm^{-1}: (b) 1650-700 cm^{-1} (c) 700-400 cm^{-1}

TABLE-3
EXPERIMENTAL FT-IR AND RAMAN AND CALCULATED
WAVENUMBERS (cm^{-1}) OF GLOBAL CONFORMATION OF PYRIDOXINE MOLECULE

Assignment This work	Experimental				This work calculated by DFT/6-311++G(d,p)					Ref. 3	Intensity		PED (≥ 5 %)
	This work		Ref. 3		Cluster		Monomer						
	IR	Ra	IR	Ra	a $\nu_{sca.}$	e $\nu_{sca.}$	$\nu_{unsca.}$ (har.)	$\nu_{sca.}$ (har.)	$\nu_{.}$ (anhar.)	ν_{unsca}	IR	Ra	
ν(OH)	3275		3850, 3950vw		3695	3691	3828	3694	3570	3823	11	76	ν(OH)(100)
ν(OH)	3167		3751vw	3476vw	3680	**3389**	3813	**3680**	3528	3822	16	18	ν(OH)(100)
ν(OH)			3170, 3282vs		**3496**	**3327**	3630	**3503**	3332	3615	100	23	ν(OH)(100)
ν(CH)	2982	3031			**3044**	**3046**	3143	**3033**	2914	3138	9	40	ν(CH)(99)
$\nu_a(CH_3)$	2952	3020			3027	3025	3135	3025	2915	3136	3	25	$\nu_a(CH_3)$(100)
$\nu_a(CH_2)$	2917	3005			3016	**3005**	3123	**3014**	2910	3122	4	16	$\nu_a(CH_2)$(99)
$\nu_a(CH_3)$	2871	2991			2974	**2976**	3078	**2970**	2852	3081	5	33	$\nu_a(CH_3)$(99)
$\nu_s(CH_2)$		2953			2944	**2959**	3050	**2943**	2828	3078	8	52	$\nu_s(CH_2)$(99)
$\nu_a(CH_2)$		2936			2936	**2950**	3039	**2933**	2811	3049	12	24	$\nu_a(CH_2)$(99)
$\nu_s(CH_3)$	2818	2921	2989s		2927	2926	3031	2925	2865	3032	7	100	$\nu_s(CH_3)$(100)
$\nu_s(CH_2)$		2884			2884	**2918**	2987	**2882**	2753	3024	19	55	$\nu_s(CH_2)$(99)
ν(CC)	1615	1618	1621, 1707w	1621w	1609	**1587**	1636	**1611**	1555	1634	4	26	ν(CC)(51)+ ν(CCC)(10)+ ν(CN)(10)
ν(CC)	1560	1565	1567m	1571w	1578	1576	1600	1576	1519	1597	5	10	ν(CC)(27)+ ν(CN)(18)+ ν(CCN)(12)
$\delta(CH_{ring})$+ ν(CC)				1465m	1505	**1471**	1524	**1501**	1446	1522	1	5	$\delta(CH_{ring})$(25)+ ν(CC)(16)+ ν(CN)(12)
δ(CCH)	1496		1441s		1500	**1449**	1520	**1497**	1424	1512	1	6	δ(CCH)(85)
$\delta(CH_2)$					1472	**1438**	1496	**1474**	1440	1495	1	5	$\delta(CH_2)$(91)
δ(CHH)	1462	1460	1413vs		1462	**1431**	1481	**1459**	1415	1480	8	8	δ(CHH)(74)
δ(CHH)	1450	1450		1385m	1457	**1429**	1477	**1455**	1405	1476	4	7	δ(CHH)(88)
δ(CCH)	1439		1359s		1428	**1394**	1448	**1426**	1377	1445	8	2	δ(CCH)(48)+ δ(CHH)(9)+ δ(CHN)(8)+ ν(CH)(7)+ ν(CN)(5)
δ(CCH)	1413	1419			1417	**1385**	1437	**1415**	1367	1410	32	13	δ(CCH)(43)+ ν(CC)(15)+ ν(CO)(10)+ δ(COH)(10)
δ(CHH)					**1396**	**1371**	1410	**1389**	1347	1407	5	11	δ(CHH)(85)
δ(CCH)	1375	1378			1376	**1347**	1397	**1376**	1321	1395	7	7	δ(CCH)(64)
δ(CCH)	1352			1326m	1364	**1338**	1383	**1362**	1313	1386	6	4	δ(CCH)(59)+ δ(COH)(28)
δ(COH)+ ν(CN)	1317	1316			1344	**1270**	1361	**1341**	1278	1372	49	8	δ(COH)(52)+ ν(CN)(21)
δ(NCH)+ ν(CN)			1287s	1279m	1293	**1264**	1313	**1293**	1247	1358	1	5	δ(NCH)(33)+ ν(CN)(15)+ ν(CC)(14)
ν(CC)	1284	1280	1251m		**1248**	**1230**	1307	**1287**	1237	1313	5	11	ν(CC)(41)+ δ(CCH)(15)+ ν(CN)(11)
ν(CC)	1251	1251	1219vs		1249	**1220**	1267	**1248**	1207	1300	6	9	ν(CC)(37)+ ν(CN)(26)+ ν(CCN)(12)
δ(CCH)	1236	1236			1243	**1207**	1261	**1242**	1195	1262	34	8	δ(CCH)(27)+ ν(CN)(14)+ ν(CO)(12)+ δ(CCN)(9)+ ν(CC)(8)
δ(CCH)	1222			1233m	1222	**1194**	1239	**1220**	1181	1251	14	11	δ(CCH)(38)+ ν(CC)(26)
δ(COH)					1211	**1187**	1228	**1210**	1166	1200	22	2	δ(COH)(54)+ δ(CCH)(22)
δ(COH)	1083		1089s		1178	**1053**	1196	**1178**	1139	1185	6	5	δ(COH)(44)+ δ(CCH)(36)
ν(CC)+ ν(CO)	1052	1054	1026vs	1059m	**1070**	**1025**	1083	**1067**	1031	1085	14	2	ν(CC)(25)+ ν(CO)(18)+ ν(CCH)(11)
δ(CCH)					1042	**1007**	1056	**1040**	1009	1055	1	0	δ(CCH)(69)+ τ(CCCN)(16)
δ(CCH)	1021				**1025**	**981**	1036	**1020**	997	1029	5	1	δ(CCH)(64)
ν(CO)					**1002**	**966**	1013	**998**	956	1012	35	16	ν(CO)(82)
ν(CO)	984	986			**992**	**954**	1003	**988**	946	1004	22	6	ν(CO)(79)
δ(CCH)			986m		985	**930**	999	**984**	952	973	8	1	δ(CCH)(50)
δ(CCH)	956	955	963m		**950**	**900**	959	**945**	923	948	1	4	δ(CCH)(45)+ ν(CC)(10)+ ν(CN)(8)
τ(CCNH)	922	928	927w		905	**887**	918	**904**	876	919	2	0	τ(CCNH)(48)+ δ(CCH)(11)
τ(CCNH)	884		882m		896	**863**	909	**895**	870	908	11	1	τ(CCNH)(38)+ τ(CCCN)(15)+ δ(CCH)(9)
τ(CCCN)	756		755s		**756**	**758**	780	**768**	756	783	1	1	τ(CCCN)(52)+ τ(CCCO)(15)+ τ(CCCC)(15)
τ(CCCN)	738	751		747w	**736**	749	762	**751**	731	763	8	2	τ(CCCN)(24)+ τ(CCCO)(15)+ δ(CCN)(20)
τ(CCOH)	692	695	692m	692vs	**710**	**729**	717	**706**	664	732	35	6	τ(CCOH)(77)
$\delta(CH_2)$+ ν(CC)			647w		**676**	**664**	681	**671**	646	683	4	27	ν(CC)(25)+ $\delta(CH_2)$(13)+ ν(CO)(10)+ τ(CCOH)(8)+ τ(CCCN)(6)
τ(CCCN)	646		575m		638	**626**	645	**635**	625	650	2	2	τ(CCCN)(35)+ τ(CCCO)(18)+ τ(CCCC)(17)
τ(CCCN)	573		552vw	544m	587	**577**	594	**585**	569	590	4	9	τ(CCCN)(39)+ τ(CCCO)(14)+ τ(CCCC)(12)

Assignment This work	Experimental				This work calculated by DFT/6-311++G(d,p)					Ref. 3	Intensity		PED (≥ 5 %)
	This work		Ref. 3		Cluster		Monomer						
	IR	Ra	IR	Ra	a $\nu_{sca.}$	e $\nu_{sca.}$	$\nu_{unsca.}$ (har.)	$\nu_{sca.}$ (har.)	$\nu_{.}$ (anhar.)	ν_{unsca}	IR	Ra	
δ(COH)	546	547			544	**532**	550	**542**	526	549	4	4	τ(CCCO)(13)+ τ(CCCN)(12)+ δ(CCN)(10)+ δ(CCC)(17)
ν(CC)+ ν(CO)	517	519	521vw	519s	520	516	528	520	506	526	3	8	δ(CCO)(22)+ δ(CCN)(12)+ δ(CCC)(26)
δ(CCH)	484	482	484vw	484m	**498**	495	502	**494**	489	505	1	6	τ(CCCN)(32)+ δ(CCCC)(21)+ δ(CCC)(19)+ δ(CHH)(6)
δ(CCH)	416	417	417w	426m	435	**425**	439	**432**	421	431	24	7	τ(CCOH)(45)+ δ(CHH)(13)+ δ(CCN)(9)
ν(CO)		391		346s	**361**	**372**	417	**411**	407	399	15	9	τ(CCOH)(52)+ δ(CCC)(5)
ν(CO)		342			**361**	360	361	**356**	351	360	7 4	8	τ(CCCN)(27)+ δ(CCO)(13) + τ(CCOH)(10) + τ(CCCO)(8)
δ(CCH)		315			**315**	**344**	316	**311**	312	358	4	0	δ(CCO)(26)+ τ(CCCN)(23)+ δ(CCC)(18)
δ(CCH)					300	**307**	304	**299**	287	320	4	9	δ(CCC)(32)+ τ(CCOH)(15)+ δ(CH_2)(8)+ δ(CCN)(6)+ τ(CCCC)(6)
τ(CCNH)		279		282m	288	292	292	288	241	291	14	10	τ(CCOH)(36)+ τ(CCCC)(14)+ τ(CCCO)(10)+ δ(CCC)(14)
τ(CCNH)					267	**276**	271	**267**	231	279	22	5	δ(CCC)(33)+ τ(CCOH)(29)+ τ(CCCC)(10)
τ(CCCN)					235	**240**	236	**232**	233	233	0	4	δ(CCC)(43)+ δ(CHH)(11)+ τ(CCCN)(10)+ τ(CCCH)(9)
τ(CCCN)				168w	215	**223**	215	**212**	211	214	2	11	τ(CCCC)(30) + τ(CCCN)(19)+ δ(CH_2)(18)+ δ(CCC)(11)
τ(CCOH)		173			**137**	**124**	133	**131**	125	131	3	14	τ(CCCN)(36)+ τ(CCCO)(28)+ τ(CCCH)(21)
δ(CH_2)+ ν(CC)				113m	**109**	116	115	**113**	113	115	0	24	τ(CCCH)(30)+ τ(CCOH)(15)+ τ(CCCC)(10)+ τ(CCCN)(10)
τ(CCCN)					**92**	**107**	98	**97**	112	97	0	14	τ(CCCH)(51)+ τ(CCOH)(16)+ τ(CCCN)(9)
τ(CCCN)					84	**89**	83	**82**	100	87	0	30	τ(CCCC)(25)+ τ(CCCN)(19)+ δ(CH_2)(15)+ τ(CCCO)(12)
τ(CCCO)					75	77	74	73	67	78	1	10	τ(CCCH)(55)+ τ(CCCO)(12)

Cluster a, pyridoxine-H_2O; Cluster e, pyridoxine-$4H_2O$; har., harmonic wavenumbers; anhar., anharmonic wavenumbers; sca., scaled; unsca., unscaled; s, symmetric; a, asymmetric

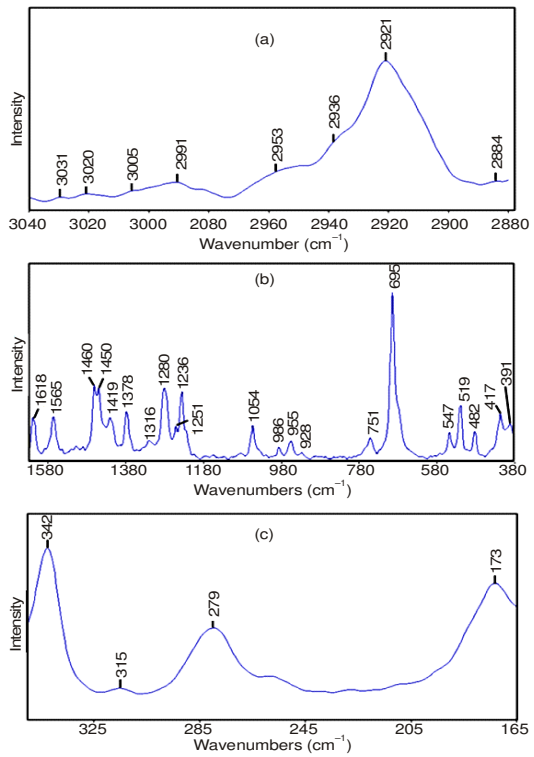

Fig. 4. Experimental Raman spectra of pyridoxine in the regions; (a) 3040-2880 cm^{-1}; (b) 1630-380 cm^{-1} (c) 350-165 cm^{-1}

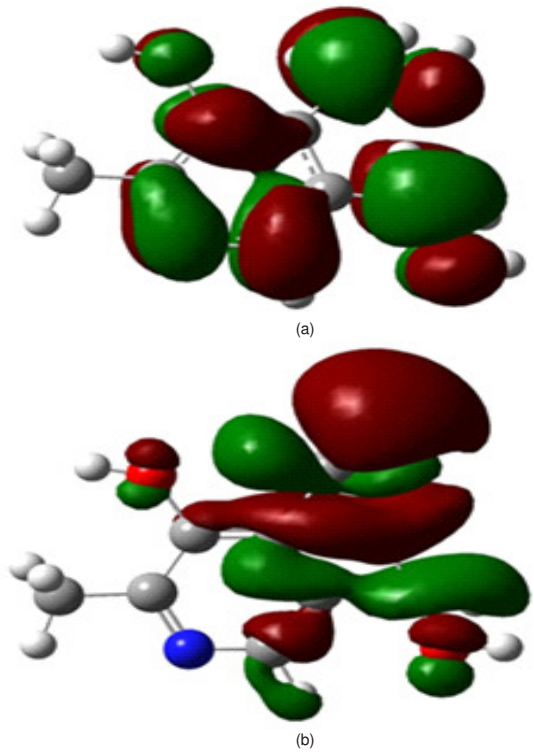

Fig. 5. HOMO and LUMO of pyridoxine

of the compound, the energies of HOMO, LUMO and HOMO-LUMO energy gaps are calculated using 6-311++G(d,p) basis set.

The calculated energies of HOMO, LUMO and HOMO-LUMO gap are -5.774, -4.774 and 1 eV, respectively. The pyridoxine molecule has a small energy gap indicating that it is a soft molecule. The soft molecules are more polarizable than the hard ones. HOMO is located over the ring, carbonyl groups, C-N bonds which are located on the ring, C-O bond which is located on the chain of the molecule. LUMO is located on the carbonyl groups and O-H bonds which are located on the chain of the molecule.

Conclusion

In this study, the monomer form and water clusters of pyridoxine were studied by using the density functional theory method at B3LYP/6-311G++(d,p) level of theory. The possible stable conformers of free pyridoxine molecule were searched by means of torsion potential energy surfaces scan studies through D1 (9H-8O-C4-3C), D2 (12H-10C-5C-6N), D3 (15O-14C-2C-1C) and D4 (O22-19H-3C-2C) which were varied from 0° to 360° by steps 10°. The H_2O complex analysis of the molecule shows behavior of pyridoxine water solution.The calculated energies of HOMO, LUMO and HOMO-LUMO gap are -5.774, -4.774 and 1 eV, respectively. The HOMO-LUMO transition implies an electron density transfer from pyridine ring to carbonyl groups and OH bonds.

ACKNOWLEDGEMENTS

This study is supported by the Research Fund of Istanbul Kultur University.

REFERENCES

1. G.S. Kiruba and M.W. Wong, *J. Org. Chem.*, **68**, 2874 (2003).
2. S. Cinta, C. Morari, E. Vogel, D. Maniu, M. Aluas, T. Iliescu, O. Cozar and W. Kiefer, *Vib. Spectrosc.*,**19**, 329 (1999).
3. M. Srivastava, P. Rani, N.P. Singh and R.A. Yadav, *Spectrochim. Acta A*, **120**, 274 (2014).
4. M.J. Frisch, G.W. Trucks, H.B. Schlegel, G.E. Scuseria, M.A. Robb, J.R. Cheeseman, G. Scalmani, V. Barone, B. Mennucci, G.A. Petersson, H. Nakatsuji, M. Caricato, X. Li, H.P. Hratchian, A.F. Izmaylov, J. Bloino, G. Zheng, J.L. Sonnenberg, M. Hada, M. Ehara, K. Toyota, R. Fukuda, J. Hasegawa, M. Ishida, T. Nakajima, Y. Honda, O. Kitao, H. Nakai, T. Vreven, J.A. Montgomery Jr., J.E. Peralta, F. Ogliaro, M. Bearpark, J.J. Heyd, E. Brothers, K.N. Kudin, V.N. Staroverov, R. Kobayashi, J. Normand, K. Raghavachari, A. Rendell, J.C. Burant, S.S. Iyengar, J. Tomasi, M. Cossi, N. Rega, J.M. Millam, M. Klene, J.E. Knox, J.B. Cross, V. Bakken, C. Adamo, J. Jaramillo, R. Gomperts, R.E. Stratmann, O. Yazyev, A.J. Austin, R. Cammi, C. Pomelli, J.W. Ochterski, R.L. Martin, K. Morokuma, V.G. Zakrzewski, G.A. Voth, P. Salvador, J.J. Dannenberg, S. Dapprich, A.D. Daniels, O. Farkas, J.B. Foresman, J.V. Ortiz, J. Cioslowski and D.J. Fox, Gaussian, Inc., Wallingford CT (2009).
5. A.D. Becke, *J. Chem. Phys.*, **98**, 5648 (1993).
6. M.J. Frisch, J.A. Pople and J.S. Binkley, *J. Chem. Phys.*, **80**, 3265 (1984).
7. K. Balci and S. Akyuz, *Vib. Spectrosc.*, **48**, 215 (2008).
8. J.M.L. Martin and C. Van Alsenoy, GAR2PED: A Program to Obtain a Potential Energy Distribution from a Gaussian Archive Record, University of Antwerp, Belgium (2007).